The tensile fatigue behaviour of a nanorubber-modified carbon fibre reinforced epoxy composite

Nazli G. Ozdemir[1*], Tao Zhang[1], Homayoun Hadavinia[1], Ian Aspin[2], Fabrizio Scarpa[3]

[1]Kingston University London, SW15 3DW, United Kingdom

[2]Cytec Industrial Materials, DE75 7SP, United Kingdom

[3]University of Bristol, BS8 1TR, United Kingdom

ABSTRACT

This study investigates the effect of nano carboxylic acrylonitrile butadiene rubber (CNBR-NP) on the tensile fatigue behaviour of carbon fibre reinforced polymer composites (CFRP) with dicyandiamide-cured epoxy matrix. The stress-controlled tension-tension fatigue behaviour at a stress ratio of R=0.1 was investigated for CFRP with neat and nanorubber-modified epoxy matrices with CNBR-NP loadings of 5, 10, 15, 20 phr. The normalised test data revealed that the high cycle fatigue lifetime of the epoxy resin modified with 15 phr of CNBR-NP was increased twice relative to the neat epoxy resin. Scanning electron microscopy (SEM) images of the fracture surfaces showed that the improved plastic deformation and energy dissipation at the fibre-matrix interface contributed towards the enhanced fatigue life of the CFRP.

Keywords: Polymer-matrix composites (PMCs); Nano particles; Fatigue; Failure criterion; Nano rubber

*Corresponding Author:

Tel: +44 (0) 7450227535, E-mail address: gulsine@yahoo.com (N.G.Ozdemir)

Present address: University of Bristol, BS8 1TR, United Kingdom

1. INTRODUCTION

Carbon fibre reinforced polymer composites (CFRP) are widely used in advanced engineering technologies such as airframe structural components, modern bicycle frames and wind turbine blades due to their high strength, lightweight and versatility. Such structures experience constant and variable-amplitude fatigue loads in service. Safe operation of these structures throughout their lifetime necessitates that they have high fracture toughness and good fatigue resistance.

The majority of engineering composite materials consist of a thermosetting epoxy matrix reinforced by continuous glass or carbon fibres. The epoxy is a highly cross-linked material and therefore features undesirable brittleness of the final composite structure, whereby the polymer has a poor resistance to crack initiation and growth that affects the overall fatigue and fracture performance of the FRP composite.

One of the ways to enhance the mechanical properties of FRPs is to improve the properties of the matrix by incorporating second phase fillers into the resin. The fatigue life enhancement and the increment in toughness are dependent upon the type of toughener used, its concentration, the size of the particles and the filler-filler and filler-matrix interactions [1-3]. An enhancement in the fatigue life of advanced composite laminates can be a potential route towards designing and manufacturing more durable composites with an extended lifetime.

Significant amount of work can be found in the literature on the effect of addition of nanorubber on the mechanical properties of epoxy resin systems [4-6]. However, there is not enough work done on the mechanical analysis of CFRP with nanorubber-toughened epoxy as matrix. Our previous work showed that the Mode I fracture

toughness increases by 250% with the addition of acrylonitrile and carboxylic acrylonitrile nanorubber to the matrix of CFRP laminates [7].

Enhancement in the fatigue behaviour of rubber particle modified epoxies has been reported in the literature [8, 5, 9]. However, to the best of our knowledge, there is no study on the tensile fatigue analysis of CFRP with nanorubber-toughened epoxy as matrix. Hence, the main aim of this investigation was to study the stress-controlled constant-amplitude tension-tension fatigue behaviour of a carbon fibre-reinforced polymeric composite (CFRP) with nanorubber-modified epoxy matrices.

This study presents the investigation on the tensile strength, tension-tension fatigue and morphological characterisation of CFRP laminates with a novel carboxylic acrylonitrile butadiene based nanorubber-toughened matrix. Epoxy matrices were toughened with nano carboxylic acrylonitrile butadiene rubber (CNBR-NP) using a laboratory-scale triple mill. Narrow particle size and even distribution was maintained in the blends using triple mill dispersion technique, which resulted in a toughened epoxy network with enhanced fatigue life.

2. EXPERIMENTAL STUDIES

The epoxy resin was liquid DGEBA (Araldite LY1556) with epoxide equivalent weight of 188 supplied by Huntsman, UK. Dicyandiamide (DICY, Dyhard D50EP) was used as the curing agent and a difunctional urone (Dyhard UR500) was used as the accelerator, both supplied by AlzChem, UK. Nano carboxylic acrylonitrile butadiene rubber (CNBR-NP) Narpow VP-501 (single particle size distribution 50-100 nm, acrylonitrile content, 26wt %), was received in powder form from SINOPEC, Beijing Research Institute of Chemical Industry (BRICI), China.

Fumed silica (FS) received from Aerosil, UK (D_{50} =1 μm) was used in the neat epoxy formulation to modify the rheological behaviour to help with CFRP laminates production. 199GSM and 2x2 Twill carbon plies from Sigmatex (UK) Ltd. (Torayca T300) were used to produce the CFRP panels. The matrix formulations used in this research work are given in Table 1.

Table 1. Formulations used in experimental work, in phr (parts per hundred of DGEBA)

CODE	DGEBA	DICY	Diurone	CNBR-NP	Fumed Silica
R/ X FS	100	14	6	-	X
X CNBR-NP/ R	100	14	6	X	-

The nanorubber was dried at ~70°C for 16 hours in an oven to eliminate the absorbed moisture. After drying, it was dispersed in DGEBA matrix and the blend was mixed at 3500 rpm for 1 minute using a DAC 150.1 FVZ speed mixer. One phr (depending on the final viscosity of the blend) of fumed silica was added to the neat epoxy matrix sample, which considerably increases the viscosity of the blends and helps to prevent the leakage of resin matrix during curing of the CFRP laminates in autoclave under high pressures.

To improve the homogeneity of the mixture, the blend was triple milled 6 times at room temperature (RT=23°C). After the mixing, the blend was magnetically stirred at a speed of 320 rpm and degassed at 70°C inside a glass flask for 16 hours under vacuum. After degassing, the curing agent and accelerator were added and the final mixture was speed mixed at 2100 rpm for 6 minutes.

Hand lay-up technique was used to produce the CFRP laminates. Bidirectional dry carbon plies $[0/0]_6$ with the nanorubber-toughened matrix were vacuum bagged and cured in an autoclave under a pressure of 6 atm. 12 layers of carbon plies were used for tensile and tensile-fatigue tests, respectively, complying with the mechanical test standards. The composite panels were heated to 120ºC at a heating rate of 0.5ºC/min and held for 1 hour at this temperature before cooling down to room temperature at the same rate. CFRP samples for mechanical testing were cut from the cured panels using high-pressure water jet.

The scanning electron microscopy (SEM) studies on the CFRP panels showed that the CNBR-NP was evenly distributed and had an average size of 50-100 nm independent of the nanorubber concentration. Further details on the characterisation of CNBR-NP/ R formulations can be found in our recent paper [10]. SEM images of the fracture surfaces of X CNBR-NP/ R matrices are given in Figure 1.
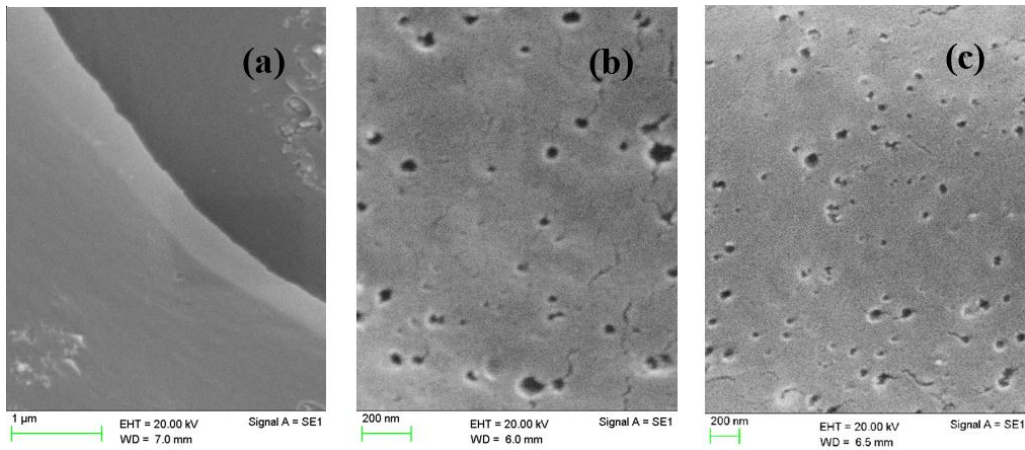

Figure 1. SEM images of the fracture surfaces of **(a)** R sample, **(b)** 5CNBR-NP/ R sample, **(d)** 20CNBR-NP/ R sample

The volume fraction of the carbon fibres in the CFRP-composites was estimated using the following equation:

$$\%V_f = \frac{W_{FAW}N_p100}{B r_F} \tag{1}$$

Where W_{FAW} is the fibre areal weight, N_p is the number of plies, B is the thickness of the CFRP panels and ρ_F is the density of the carbon fibre. The value of W_{FAW} is quoted from the manufacturer's datasheet of the carbon fabrics, (199 g/m^2). The density of the high strength carbon fibre is 1.76 g/cm^3. The mean values of the thicknesses of the CFRP panels measured using a digital micrometre and the carbon fibre volume fractions are shown in Table 2. CFRP panels with the highest nanorubber concentrations (15 CNBR-NP/ R and 20 CNBR-NP/ R matrices) have the lowest carbon fibre volume fraction and the volume fraction differs significantly by 8%.

The tensile properties, including the ultimate tensile strength UTS, and modulus E_1, of the test specimens, determined in compliance with the ASTM D3039 standard using three replicates, are shown in Table 2.

Table 2. Mean thickness, B, and estimated fibre volume fraction, V_f, of the CFRP-composites with neat and X CNBR-NP/ R matrices, SD = Standard deviation

X	Specimen thickness, B (mm)	V_f	UTS (MPa)		E (GPa)	
			Mean	SD	Mean	SD
R/ 1FS	2.7 (±0.1)	0.50	661	24	58.2	4.2
5	2.6 (±0.15)	0.52	696	20	58	5.1
10	2.6 (±0.18)	0.53	645	18	55.9	3.2
15	2.8 (±0.14)	0.48	561	22	53.1	4.3
20	3.0 (±0.7)	0.45	531	32	53.9	5.3

Stress-controlled tension-tension fatigue tests of CFRP specimens were performed at RT (23°C) with servo hydraulic Zwick Roell 25kN equipment using a sinusoidal wave load. The ratio of the minimum cyclic stress to the maximum cyclic stress, i.e., the R-ratio, was 0.1. A cyclic frequency of 5 Hz was used and the sample dimensions were $250 \times (10\pm2) \times (3\pm0.2)$ mm. Aluminium end tabs were used to reduce possible stress concentration resulting from high gripping pressure. Three tests were performed for each formulation at each stress level.

During the tests the number of cycles to failure was recorded, as well as the maximum and minimum displacements. The results were analysed in terms of stress range versus the number of cycles to failure, i.e., by representation of data as S–N Wohler curves.

The load vs. displacement data for one complete fatigue cycle was analysed at regular intervals during the fatigue test, and the sample stiffness was calculated [11]. 50 points of load/displacement data in the central position of the rising half of the fatigue cycle were used to perform the regression analysis. Normalised stiffness of the specimen was defined as the ratio of the measured stiffness at any given fatigue cycle to the initial stiffness in the first cycle.

The fracture surfaces of the fatigue test specimens were observed using scanning electron microscopy (SEM) at secondary electron mode. The samples were vacuum coated with gold using a sputter coater. Images were taken using an accelerating voltage of 20-25 keV with a magnification between 90 times and 2000 times.

3. RESULTS AND DISCUSSION

Figure 2 (a) and (b) show the tensile stress-strain curves of the CFRP panels. All specimens failed immediately after the tensile stress reached the maximum value. This

type of premature failure indicates a damage mechanism that is observed in panels that consist of a brittle matrix and high modulus carbon fibre (Figure 2 (c)). In such type of laminates, strain cannot be efficiently transferred from the high modulus fibres to the low modulus matrix, resulting in a brittle failure as can be seen in Figure 2 (d) and (e).
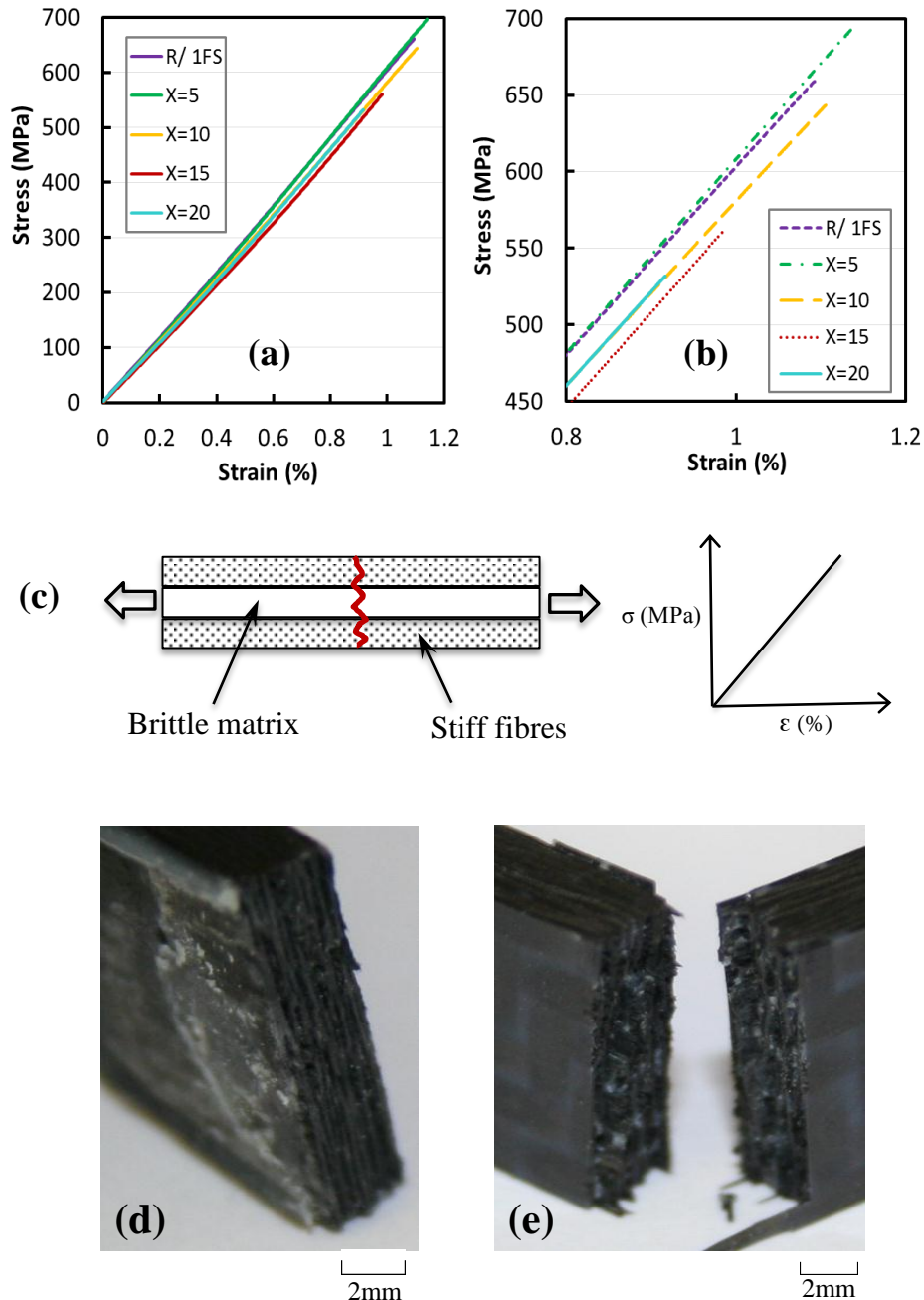

Figure 2. (a), (b) Tensile stress-strain curves of CFRP panels with X CNBR-NP/ R matrices, (c) Damage mechanism resulting in a premature failure [18], (d) tensile fatigue fracture surface of CFRP with R/ 1FS matrix (σ_{max} = 563 MPa), and (e) 20CNBR-NP/ R matrix (σ_{max} = 530 MPa)

The stress-controlled, constant amplitude, cyclic-fatigue test results for the CFRP panels are given in Figure 3. This figure shows the effect of CNBR-NP on the fatigue life by depicting the stress-number of cycles to failure (*S-N*) curve. It revealed that the fatigue life of the composite with the neat epoxy matrix was extended by 55% with the addition of 5 phr of CNBR-NP to the matrix of the CFRP panel. However, with further addition of nanorubber to the matrix, the fatigue life was shortened at every stress level. This is mainly attributed to the reduction in the tensile strength of the nano-modified CFRP panels with further integration of nanorubber into the matrix (Table 2).

The experimental data of stress vs. number of cycles to failure (*S-N* curves) for the CFRP panels was fitted to Basquin's law [12]:

$$S = S_f (N_f)^b \tag{2}$$

Where S_f is the fatigue strength coefficient (FSC), and b is the fatigue strength exponent (FSE). The values of the FSC and FSE determined for the CFRP with neat and nanoparticle-modified matrices are given in Table 3.

Addition of 5 phr of CNBR-NP to the matrix of the composites increased the FSC and decreased the FSE by 4% and 15%, respectively. This means that the panel with 5 CNBR-NP/ R matrix exhibited the highest fatigue performance. However, the characteristic fatigue properties did not show a great variance. In Table 3, the equations for the characteristic fatigue lines of the composite samples are listed. A consistent decrease in the slope of the nanorubber-modified samples is noticeable above 5 phr of CNBR-NP loading. This indicates that the composites with the nanorubber-modified matrices endure more cycles at lower stresses. Hence, the nanorubber is even more effective at low stress levels. This effect may be explained by the failure mechanisms in

9

carbon fibre composites subjected to cyclic loading. Fatigue life of carbon fibre composites is related to the nucleation and growth of damage in the polymer matrix. At high cyclic stress levels, significant matrix damage is created in a few cycles. At low cyclic stress levels, damage in the matrix is limited and with continued cycling, a few cracks propagate slowly until failure occurs.

Improvement in tensile strength and fatigue performance is often explained by higher matrix strength and fibre/ matrix interface strength. In this research, the main reason of the difference in the tensile and fatigue properties of the CFRP panels (Figure 3) was the carbon fibre volume fraction (V_f) of the panels. V_f was 0.52 for the CFRP panel with 5 CNBR-NP/ R matrix which resulted in a slight increase in the tensile strength and hence relatively higher number of cycles till fracture for the tension-tension fatigue tests.
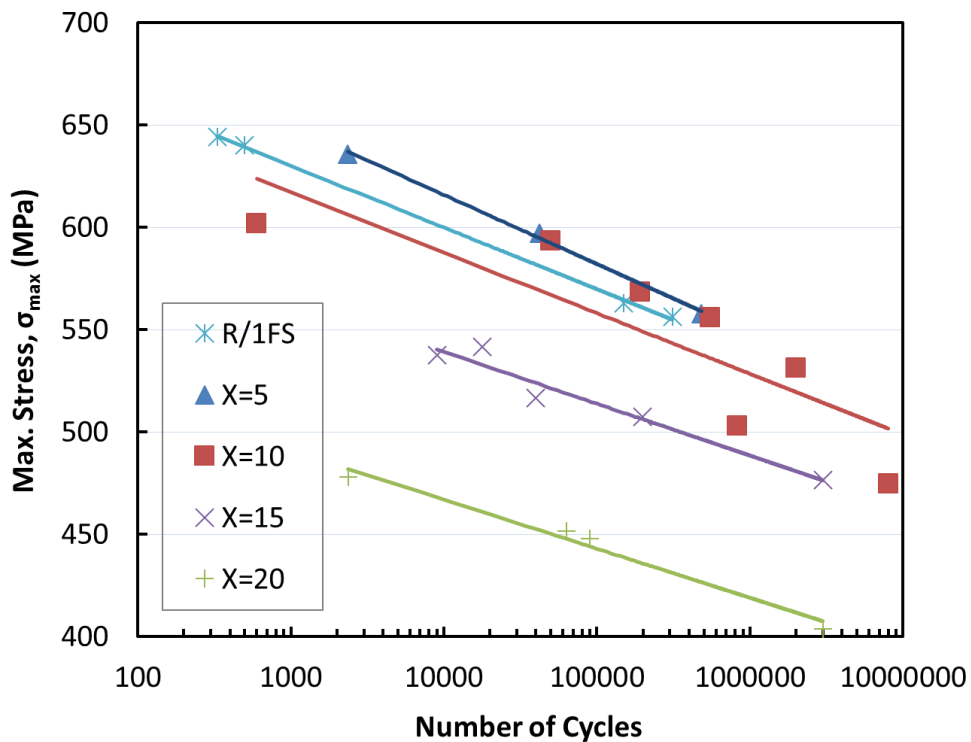

Figure 3. Stress versus lifetime (*S-N*) curves of the CFRP panels with R/ 1FS and X CNBR-NP/ R matrices

Table 3. Fatigue properties of the CFRP panels with R/ 1FS and X CNBR-NP/ R matrices

X	Equation	Fatigue properties	
		FSC (MPa)	FSE
R/ 1FS	$\sigma = 721(N_f)^{-0.020}$	721	-0.020
5	$\sigma = 751(N_f)^{-0.023}$	751	-0.023
10	$\sigma = 706(N_f)^{-0.018}$	706	-0.018
15	$\sigma = 641(N_f)^{-0.018}$	641	-0.018
20	$\sigma = 563(N_f)^{-0.019}$	563	-0.019

In addition to standard tensile test, tensile strength for different specimens was determined from the fatigue tests by extrapolating the *S-N* curves (Figure 3) to intersect the y-axis. The results are represented in Figure 4. In this figure, the trend in the tensile strength deduced from the *S-N* curves is very consistent with that of the standard tensile test data. It can be seen that the tensile fatigue test data is higher than the tensile test data at all nanorubber concentrations. The reason of the ~40 MPa difference (Figure 4) between the two UTS data can be attributed to the gripping stress acting on the samples and the different testing conditions. Aluminium end tabs were not used when testing the CFRP panels under standard tensile tests, initiating high stress concentration due to gripping pressure of the hydraulic tensile testing machine. Hence, the samples broke close to the gripping ends with slightly lower tensile strength.
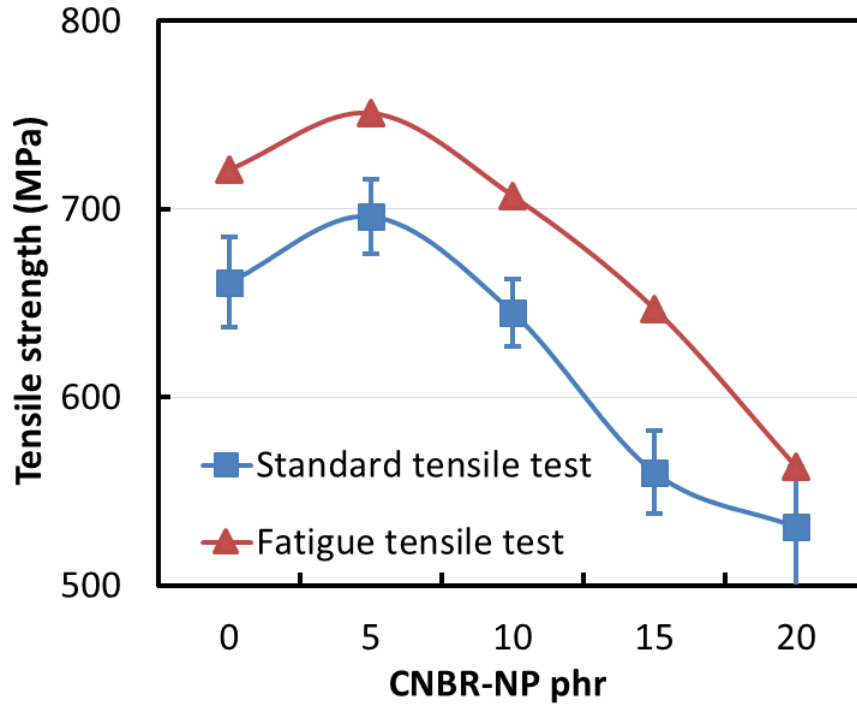
Figure 4. Tensile strength vs. CNBR-NP phr (Tensile fatigue test data for N=1)

The normalised *S-N* curves for the neat and the CNBR-NP modified CFRP panels are shown in Figure 5. A close proximity is observed between the *S–N* curves of the CFRP panel with the neat resin matrix and of the CFRP panels with the nanorubber modified matrices; suggesting that under tension–tension fatigue loading the nanorubber addition does not significantly affect the performance of the composites. This is attributed to the damage mechanism observed in such laminates that consist of a high modulus fibre and a low modulus matrix. As the tensile stress-strain curves (Figure 2 (a)) of these panels suggest; the strain in the carbon fibres cannot be efficiently transferred to the matrix, preventing the contribution of the matrix to the fatigue behaviour of the panels.
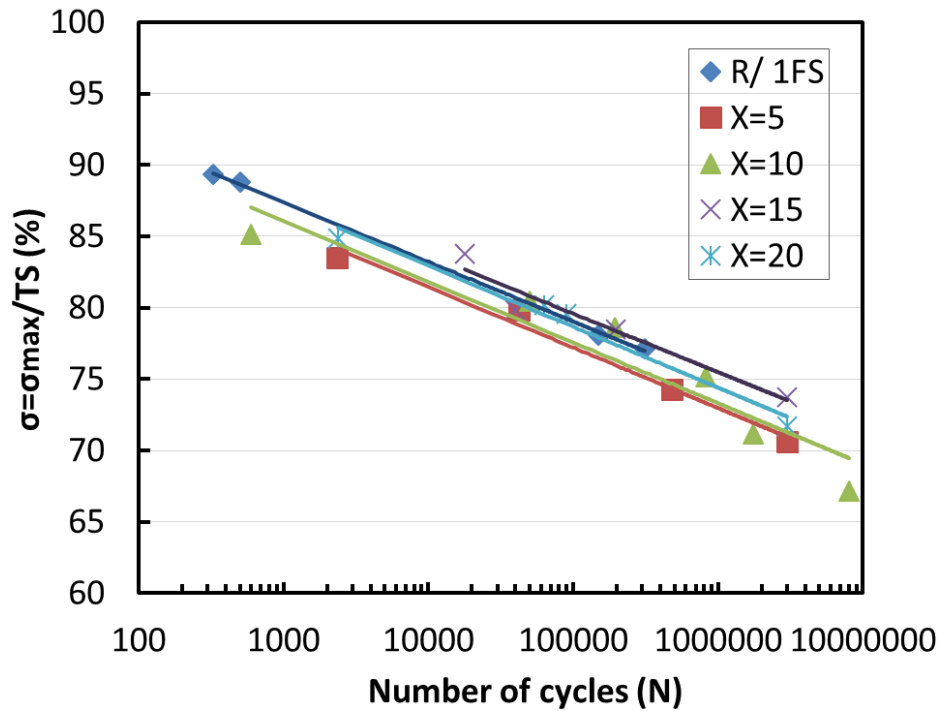
Figure 5. Normalised *S-N* curves for CFRP panels with neat and X CNBR-NP/ R matrices

In Figure 5, the samples with the matrices R/ 1FS, 15CNBR-NP/ R and 20CNBR-NP/ R performed very similar. The results reveal that the fatigue life was extended by 32% in the CFRP panel with 15CNBR-NP/ R matrix, when compared to the CFRP panel with the neat matrix at 80% normalized ($\sigma=\sigma_{max}$/TS, %) cyclic stress.

Table 4 lists the normalised experimental data. It is interesting to see that the sample with 15CNBR-NP/ R matrix performs very similar to the other samples at applied maximum stresses of 80 and 85% UTS, however its fatigue life was extended by almost twice at maximum applied stress of 75% UTS. Thus, it could be concluded that the high cycle fatigue was enhanced in the panel with 15CNBR-NP/ R matrix.

Table 4. UTS Normalised experimental data for the CFRP with neat and X CNBR-NP/ R matrices

Maximum cyclic stress, %UTS	Number of cycles to failure, CFRP with X CNBR-NP/ R matrix				
	R/ 1FS	X=5	X=10	X=15	X=20
75	923,753	332,154	400,312	1,794,074	724,111
80	58,860	21,983	26,804	78,826	48,604
85	3750	1457	1794	4662	3262

The normalised stiffness variation with the number of cycles, evaluated for the fatigue tests at σ_{max}=640 MPa for the CFRP panels with R/ 1FS and 5CNBR-NP/ R matrices is shown in Figure 6. In general, materials exhibit stiffness reduction with fatigue cycles [13, 14]. It may be noted that the initial stiffness reduction for both samples is significant, however, rate of this reduction was slightly higher for the CFRP panel with 5CNBR-NP/ R matrix. This may be attributed to the deeper slope of the CFRP panel with 5CNBR-NP/ R matrix when compared to the panel with the neat matrix (Table 3). The trend in the stiffness reduction is directly related to matrix cracking and correlates well with the slope of the *S-N* curves of these panels.
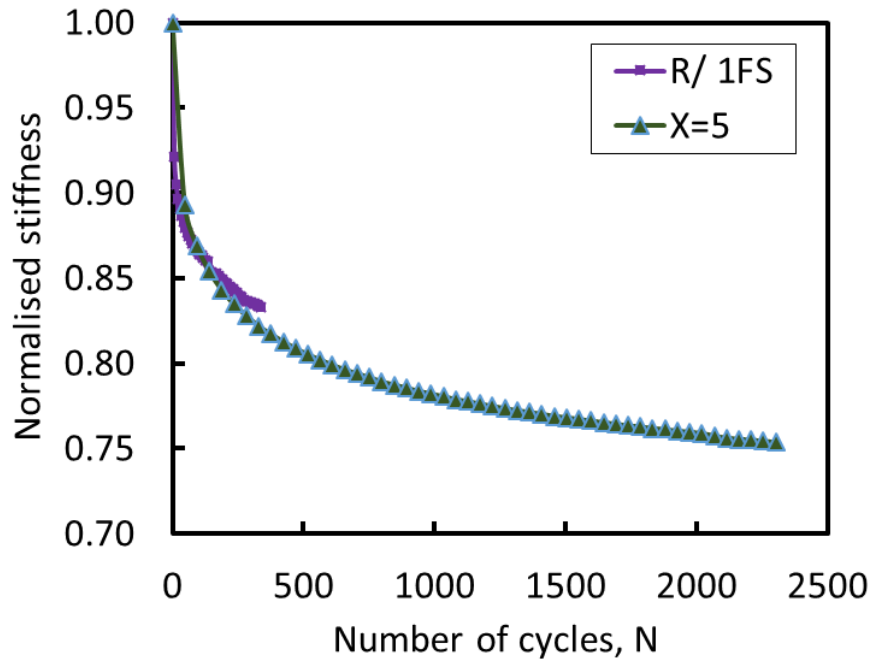
Figure 6. Normalised stiffness vs. number of cycles for CFRP panels with R/ 1FS and 5 CNBR-NP/ R matrices (σ_{max}=640 MPa, R=0.1).

Figure 7 illustrates the SEM images of the fracture surfaces of the CFRP panels after fatigue failure. Fibre breakage, interface debonding and delamination were observed in the CFRP panels with both neat and nanorubber-toughened matrices.

In Figures 7 (a) and (b), the damage mechanisms of the laminate with the neat matrix consisted of debonding at the fibre-matrix interfaces and fracture of axial fibres. Debonding at the axial fibre-matrix interfaces occurred as a result of local stresses that develop at the interfaces during loading. This debonding was correlated with individual axial fibres becoming overloaded prematurely and fracturing [15]. As fibres subsequently continue to fracture prematurely it causes stress concentrations and local stresses at the interface is developed. High amount of fibre pull-out resulting from weak fibre-matrix interfacial strength is easily noticeable in the panel with the neat matrix

(Figure 7 (a)). The neat epoxy shows a relatively smooth fracture surface, devoid of any indications of large-scale plastic deformation.

In Figures 7 (b) and (d), extrusion of carbon fibres on the smooth fracture surface are clearly observable, implying that the adhesion between the carbon fibres and the matrix is weak in the sample with 5 CNBR-NP/ R matrix. Consequently, the carbon fibre debonded from the matrix under cyclic loading, causing severe delamination.

In Figures 7 (e) and (g), for the panels with relatively higher nanorubber concentration matrices, high amount of plastic deformation at the fibre-matrix interface, which may have acted as an energy dissipation mechanism, indicated an improved interfacial toughness. This suggests that the CNBR-NP developed a resistance to fibre-matrix failure. This is attributed to the creation of an interphase between the fibre and matrix that can be clearly seen in Figure 7 (f). In Figures 7 (g) and (h), in the sample with 20CNBR-NP/ R matrix, lotus leaf formation was observed which is another type of damage mechanism mainly resulting from good adherence of the fibres to the matrix.
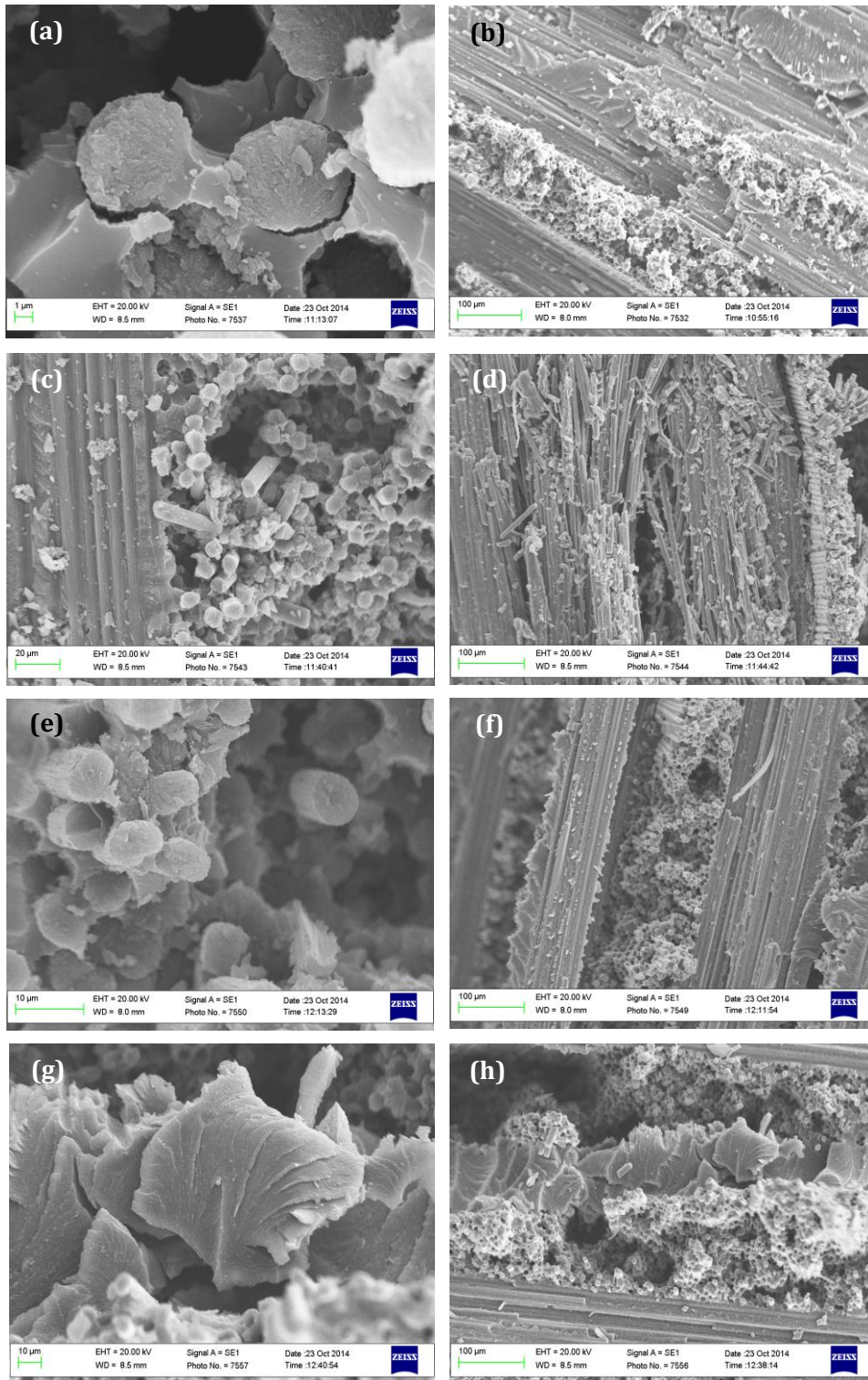
Figure 7. SEM images of the fracture surfaces of the CFRP panels tested in tensile fatigue, **(a)**, **(b)** laminates with R/ 1FS matrix, **(c), (d)** laminates with 5 CNBR-NP/ R matrix, **(e), (f)** laminates with 15 CNBR-NP/ R matrix, **(g), (h)** laminates with 20 CNBR-NP/ R matrix

17

Figure 8 is a close-up SEM image showing the axial fibre-matrix interface of the CFRP panels. The most distinctive differences in the fracture surfaces of these two laminates were the extent of fibre pull-out and the plastic deformation close to the interface. Although there was clear plastic deformation in the laminate with 15CNBR-NP/ R matrix when compared to the smooth and glassy fracture surface of the laminate with the neat resin matrix, neither the tensile strength, nor the fatigue performance was strongly affected by CNBR-NP modification of the matrix. This may be due to the fibre-dominated nature of the tensile and fatigue properties of the composites.
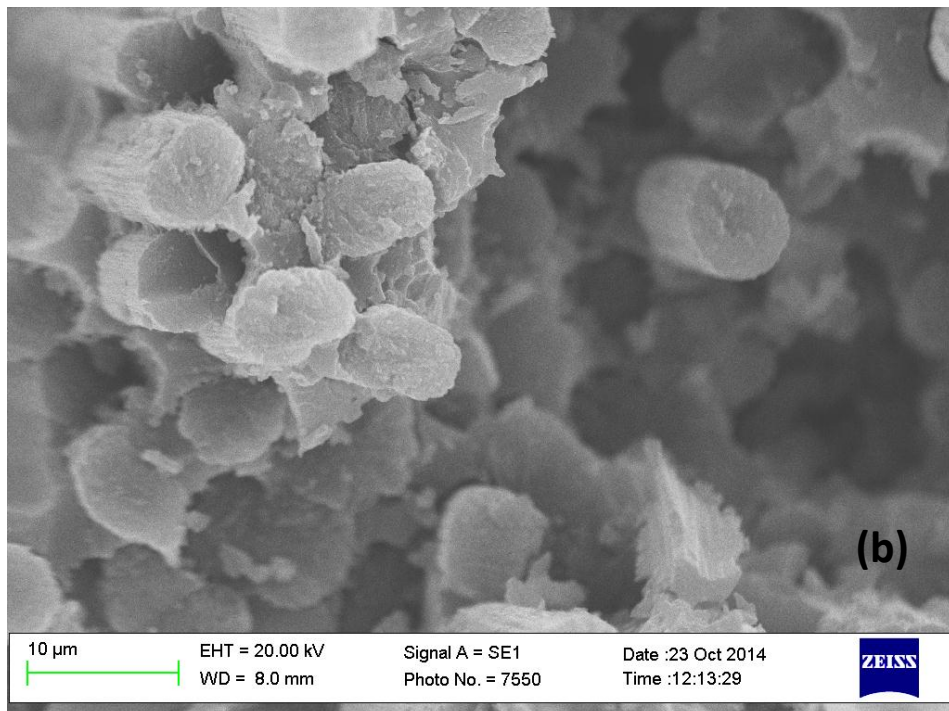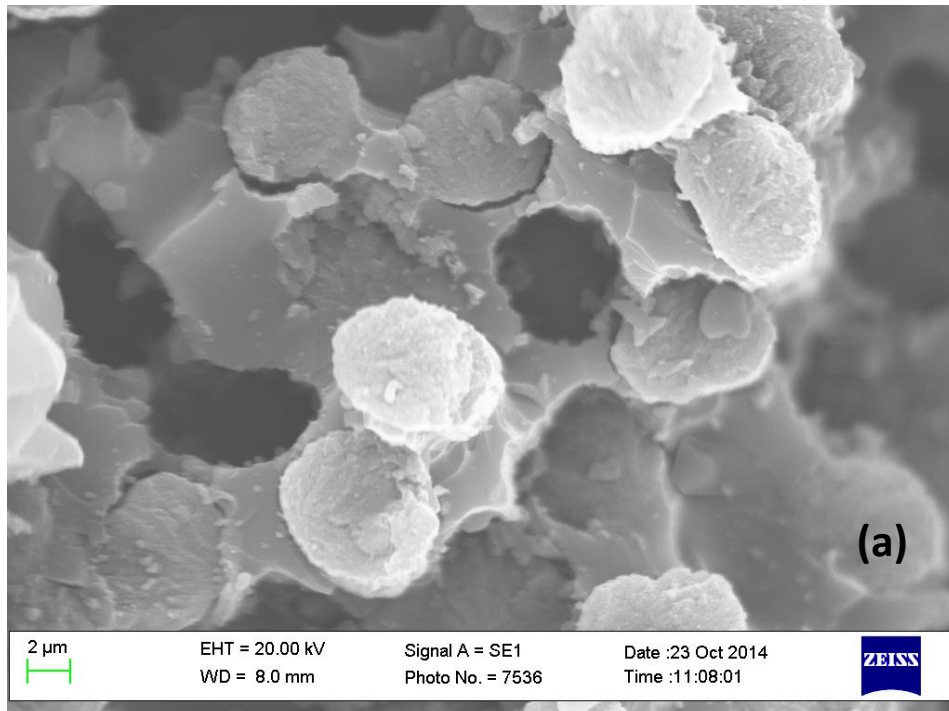
Figure 8. SEM images of the fracture surfaces of the CFRP panels tested in tensile fatigue, **(a)** laminate with R/ 1FS matrix, **(b)** laminate with 15 CNBR-NP/ R matrix

4. CONCLUSIONS

The following conclusions can be drawn based on the results obtained in this investigation.

1. Unlike in the low-modulus glass fibre composites [16], the high moduli of the carbon fibres prevent the imposition of strains in the matrix and hence inhibit the matrix fatigue failure. The specimens rather fail in fibre and the matrix modification does not have a significant effect on the fatigue behaviour of the laminates at low cycle fatigue.

2. Normalised test data revealed that the high cycle fatigue life was enhanced by twice in the CFRP panel with 15 CNBR-NP/ R matrix. Nanorubber toughening of resin can improve the energy dissipation capacity of the matrix and the extent of plastic deformation at the interface. Hence, the modified matrix can act as a stress relief medium, resulting in improved strain transfer between the fibre and the matrix phase and an enhanced fatigue life.

REFERENCES

[1] C. Manjunatha, A. Taylor, A. Kinloch and S. Sprenger, "The effect of rubber micro-particles and silica nano-particles on the tensile fatigue behaviour of a glass-fibre epoxy composite," *J Mater Sci,* vol. 44, pp. 342-345, 2009.

[2] N. T. Phong, M. H. Gabr, K. Okubo, B. Chuong and T. Fujii, "Improvement in the mechanical performances of carbon fiber/epoxy composite with addition of nano-(Polyvinyl alcohol) fibers," *Composite Structures,* vol. 99, pp. 380-387, 2013.

[3] Y. Zhou, F. Pervin, S. Jeelani and P. Mallick, "Improvement in mechanical properties of carbon fabric-epoxy composite using carbon nanofibers," *Journal of materials processing technology,* vol. 198, pp. 445-453, 2008.

[4] G. Qi, X. Zhang, B. Li, S. Zhihai and J. Qiao, "The study of rubber-modified plastics with higher heat resistance and higher toughness and its application," *Polymer chemistry,* vol. 2, pp. 1271-1274, 2011.

[5] A. Kinloch, S. Lee and A. Taylor, "Improving the fracture toughness and the cyclic-fatigue resistance of epoxy-polymer blends," *Polymer,* vol. 55, no. 24, pp. 1-10, 2014.

[6] Y. Zhao, Z.-K. Chen, Y. Liu, H.-M. Xiao, Q.-P. Feng and S.-Y. Fu, "Simultaneously enhanced cryogenic tensile strength and fracture toughness of epoxy resins by carboxylic nitrile-butadiene nano-rubber," *Composites Part A: Applied Science and Manufacturing,* vol. 55, p. 178–187, 2013.

[7] N. G. Ozdemir, T. Zhang, H. Hadavinia and I. Aspin, "Toughening of carbon fibre reinforced polymer composites with nanorubber for advanced industrial

applications," *Materials and design,* 2015.

[8] C. M. Manjunatha and A. C. Taylor, "The cyclic-fatigue behaviour of an epoxy polymer modified with micron-rubber and nano-silica particles," *Journal of materials science,* vol. 44, pp. 4487-4490, 2009.

[9] H.-Y. Liu, G. Wang and Y.-W. Mai, "Cyclic fatigue crack propagation of nanoparticle modified epoxy," *Composites Science and Technology,* vol. 72, no. 13, p. 1530–1538, 2012.

[10] N. G. Ozdemir, T. Zhang, H. Hadavinia, I. Aspin and J. Wang, "Rheological properties, cure characteristics, and morphology of acrylonitrile-based nanorubber modified epoxy," *Journal of applied polymer science,* 2015.

[11] K. F. J. Y. J. Lee, "Prediction of fatigue damage and life for composite laminates under service loading spectra," *Compos Sci Technol,* vol. 56, p. 635–648, 1996.

[12] A. Buch, *Fatigue strength calculation,* Switzerland: Transtech publications, 1988.

[13] W. Boukharouba, A. Bezazi and F. Scarpa, "Identification and prediction of cyclic fatigue behaviour in sandwich panels," *Measurement,* vol. 53, pp. 161-170, 2014.

[14] C. Manjunatha, R. Bojja and N. Jagannathan, "Fatigue behavior of a nanocomposite under a fighter aircraft spectrum load sequence," *Journal of nano research,* vol. 24, pp. 58-66, 2013.

[15] J. Zhu, A. Imam, R. Crane and K. Lozano, "Processing a glass fiber reinforced vinyl ester composite with nanotube enhancement of interlaminar shear strength," *Composites Science and Technology,* vol. 67, no. 7-8, p. 1509–1517, 2007.

[16] C. Manjunatha, R. Bojja and N. Jagannathan, "Fatigue behavior of a nanocomposite under a fighter aircraft spectrum load sequence," *Journal of nano research,* vol. 24, pp. 58-66, 2013.

[17] E. Gamstedt and B. Sjogren, "Micromechanism in tension-compression fatigue of composite laminates containing transverse plies," *Composites science and technology,* vol. 59, pp. 167-178, 1999.

[18] M. Jalalvand, "Damage analysis of pseudo-ductile thin-ply UD hybrid composites – A new analytical method," *Composites Part A: Applied Science and Manufacturing,* vol. 69, p. 83–93, 2015.